

See discussions, stats, and author profiles for this publication at: <https://www.researchgate.net/publication/49760649>

Optical imaging of excited-state tautomerization in single molecules

ARTICLE *in* PHYSICAL CHEMISTRY CHEMICAL PHYSICS · FEBRUARY 2011

Impact Factor: 4.49 · DOI: 10.1039/c0cp02228d · Source: PubMed

CITATIONS

23

READS

50

10 AUTHORS, INCLUDING:



[Regina Jäger](#)

University of Tuebingen

7 PUBLICATIONS 35 CITATIONS

[SEE PROFILE](#)



[Hans-Georg Mack](#)

University of Tuebingen

152 PUBLICATIONS 2,136 CITATIONS

[SEE PROFILE](#)



[Michael Hanack](#)

University of Tuebingen

715 PUBLICATIONS 11,811 CITATIONS

[SEE PROFILE](#)



[Alfred J. Meixner](#)

University of Tuebingen

228 PUBLICATIONS 3,563 CITATIONS

[SEE PROFILE](#)

Cite this: *Phys. Chem. Chem. Phys.*, 2011, **13**, 1722–1733

www.rsc.org/pccp

PERSPECTIVE

Optical imaging of excited-state tautomerization in single molecules†

Anna M. Chizhik,^a Regina Jäger,^a Alexey I. Chizhik,^a Sebastian Bär,^a Hans-Georg Mack,^a Marcus Sackrow,^a Catrinel Stanciu,^a Alexey Lyubimtsev,^b Michael Hanack^b and Alfred J. Meixner^{*a}

Received 21st October 2010, Accepted 4th January 2011

DOI: 10.1039/c0cp02228d

Tautomerism process of single fluorescent molecules was studied by means of confocal microscopy in combination with azimuthally or radially polarized laser beams. During a tautomerism process the transition dipole moment (TDM) of a molecule changes its orientation which can be visualized by the fluorescence excitation image of the molecule. We present experimental and theoretical studies of two porphyrazine-type molecules and one type of porphyrin molecule: a symmetrically substituted metal-free phthalocyanine and porphyrin, and nonsymmetrically substituted porphyrazine. In the case of phthalocyanine the fluorescence excitation patterns show that the angle between the transition dipole moments of the two tautomeric forms is near 90°, in agreement with quantum chemical calculations. For porphyrazine we find that the orientation change of the TDM is less than 60° or larger than 120°, as theoretically predicted. Most of the porphyrin molecules show no photoinduced tautomerization, while for 7% of the total number of investigated molecules we observed excitation patterns of two different *trans* forms of the same single molecule. We demonstrate for the first time that a molecule, undergoing a tautomerism process stays in one tautomeric *trans* conformation during a time comparable with the acquisition time of one excitation pattern. This allowed us to visualize the existence of each of the two *trans* forms of one single porphyrin molecule, as well as the sudden switching between these tautomers.

^a Institute of Physical and Theoretical Chemistry,
University of Tübingen, Auf der Morgenstelle 18, 72076 Tübingen,
Germany. E-mail: alfred.meixner@uni-tuebingen.de

^b Institute of Organic Chemistry, University of Tübingen,
Auf der Morgenstelle 18, 72076 Tübingen, Germany

† Electronic supplementary information (ESI) available. See DOI:
10.1039/c0cp02228d

1. Introduction

Tautomerization is a basic chemical process, attracting research interest for several decades. Specific chemical and especially biochemical reactions require modification in the constitution of the molecules. Prototropy is the most important



Anna M. Chizhik

Anna M. Chizhik received BSc and MSc degrees in physics from Saint-Petersburg State University in 2007 (Saint-Petersburg, Russia). Her graduate studies were concentrated on FTIR investigation of HCN on oxide adsorbents. She carried out her doctoral work at the Institute of Physical and Theoretical Chemistry, University of Tübingen under the supervision of Prof. Alfred J. Meixner and received her PhD in 2010. Her research interests include imaging of

single quantum emitters and determination of their transition dipole moment orientation and dimensionality using higher order laser modes.



Regina Jäger

Regina Jäger started as a scientific assistant in the group of Professor Alfred J. Meixner at the University of Tübingen during her study in 2005. She received her diploma in chemistry in 2009. During her graduate studies she was investigating tautomerization of single octaethylporphyrin molecules. She is currently a PhD student at the group of Prof. Alfred J. Meixner, University of Tübingen. Her research interests include optical microscopy and spectroscopy of single quantum emitters like organic dye molecules and rare earth nanoparticles as well as optical trapping.

tautomerism, which occurs in nature. Many porphyrin derivatives can be found in a complex bound to a metal ion, *e.g.* in hemoglobin for oxygen transportation or in chlorophyll for photosynthesis. Phthalocyanines are widely used as blue or green pigments for ink- and laser-printers and like porphyrazines and porphyrins in photodynamic tumortherapy (PDT).^{1–5} Moreover, light-induced tautomerization can be used for information storage in holography.⁶ Porphyrins serve as biomimetic models for enzymes, for catalytic reactions, as well as sensors and biosensors.⁷ For the investigation of the tautomerism process porphyrin molecules can be considered as a basic matrix for prototropy, since it proceeds isolated in the inner ring of the symmetric structure of the porphyrin.

Tautomerism processes have been intensively studied by nuclear magnetic resonance (NMR) analysis,^{8,9} combined with isotope markers, insertion of different substituents to investigate the tautomerism process in porphyrin systems in solutions as well as in crystals at low and high temperatures.^{10–15}

It should be noted that NMR studies provide information only on the ground state tautomerism process. Other spectroscopic methods, such as fluorescence spectroscopy,¹⁶ polarization spectroscopy,^{17,18} as well as influences of excitation by studying near-infrared two-photon absorption spectra¹⁹ and other experiments involving excited states concerning photoisomerism^{20,21} have also been used to investigate tautomerization. In agreement with experimental results, theoretical studies of porphyrin molecules and their derivatives revealed two possible intramolecular processes: a synchronous hydrogen movement, *i.e.* transition between two *trans* states, or a step-wise transition through a *cis* tautomer.^{9,10,22} Previous researchers showed that one of the inner hydrogens can move and form the *cis* tautomer.^{8,13–15,20,21} Afterwards the initial *trans* form can be reproduced again or the other hydrogen can change its position relaxing into the chemically identical *trans* tautomer, but with a different position of the hydrogen atoms. Nevertheless, these methods can provide only averaged information for an ensemble of molecules.



Alexey I. Chizhik

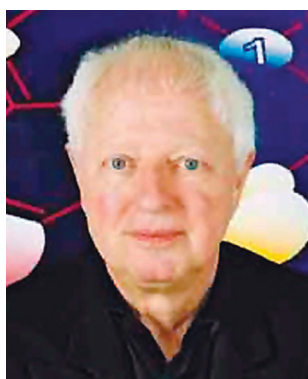
Alexey I. Chizhik received his BSc and MSc degrees in physics from Saint-Petersburg State University in 2008 (Saint-Petersburg, Russia). His diploma thesis was focused on the investigation of adsorbed species using the method of FTIR spectroscopy. He is currently doing his doctorate at the Institute of Physical and Theoretical Chemistry, University of Tübingen and works under the supervision of Prof. Alfred J. Meixner. His research interests focus on modification of emission of single organic dye molecules placed inside an optical tunable microresonator, photoluminescence of individual semiconductor nanocrystals and SiO₂ nanoparticles.

interests focus on modification of emission of single organic dye molecules placed inside an optical tunable microresonator, photoluminescence of individual semiconductor nanocrystals and SiO₂ nanoparticles.



Hans-Georg Mack

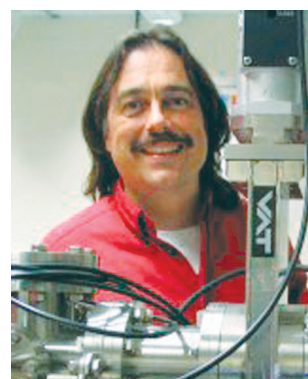
*Hans-Georg Mack received his PhD from Eberhard Karls University of Tübingen (Germany) under the supervision of Prof. Heinz Oberhammer. After finishing his habilitation he obtained the ‘Venia Legendi’ for Physical Chemistry in 1994. He is currently working as Senior Scientist at the Department of Physical and Theoretical Chemistry at Tübingen University. His research interests in the field of Computational Chemistry are focused on structures, conformations, IR/Raman spectra, tautomerization processes and excited electronic states of macrocyclic organic molecules, *e.g.* phthalocyanines, porphyrins and related compounds.*



Michael Hanack

Michael Hanack finished his graduate work in 1957. In 1970 he became full Professor of organic chemistry and Head of the Department of Organic Chemistry at the University of Saarbrücken. Since 1975 he has worked at the University of Tübingen. Prof. Hanack is one of the editors of the standard synthesis handbook Houben-Weyl, Methods in Organic Chemistry and one of the editors of the journal Synthetic Metals. Prof. Hanack has published more than 670 papers and supervised more than 230 students. His research interests cover a broad range of studies in the field of organic chemistry.

His research interests cover a broad range of studies in the field of organic chemistry.



Alfred J. Meixner

Alfred J. Meixner received his diploma in chemistry in 1984 and his PhD in 1988 from the Swiss Federal Institute of Technology (ETH) and has been a World Trade Fellow at the IBM-Almaden Research Centre. He earned his habilitation in physics from the University of Basel (Switzerland) and is currently full professor of physical chemistry and director of the Institute of Physical and Theoretical Chemistry at the Eberhard Karls University Tübingen. His research interests are optical single-molecule spectroscopy, near-field optical microscopy and quantum optics.

The combination of confocal microscopy with cylindrical vector beams (azimuthally and radially polarized doughnut modes, APDM and RPDM, respectively) is widely used for the investigation of single quantum emitters. This method provides information about the excitation transition dipole moment (TDM) while other microscopy techniques, *e.g.* defocusing imaging^{23,24} or polarization microscopy,²⁵ provide information about the emission TDM. The knowledge of the orientation of a molecule's TDM is directly related to the orientation of the molecule. Thus, the relative position of a certain molecule can be obtained with respect to the sample plane. The optical imaging of the excitation patterns has already been employed to the analysis of tautomerization in single porphycene molecules by Piwonski *et al.*^{26,27} Since the *trans* forms are chemically and magnetically equal, single molecule confocal microscopy provides a new insight into the excited-state tautomerism process, while other techniques are not able to discriminate between these two forms.

In the present perspective review we show new results of the experimental and theoretical investigations of the tautomerism process in a symmetrically substituted metal-free phthalocyanine (H_2Pc), an asymmetrically substituted porphrazine and a symmetric octaethylporphyrin (OEP). Single molecule studies have been carried out using higher order laser modes (APDM and RPDM),^{28–34} also known as cylindrical vector beams, in combination with confocal microscopy.^{35,36} This method allows us to do imaging of the tautomerism process at the single molecule level and moreover, to determine the three-dimensional orientation of the molecule's TDM upon its reorientation due to the tautomerism process by comparing experimental and simulated excitation patterns. The molecules were investigated on glass cover slides, in a polar or nonpolar polymer matrix to exclude movement, rotation or any effects of polarity. We have found that the phthalocyanine and porphrazine molecules exhibit a tautomerism process, which results in fast switching (faster than the scan speed in the optical measurements) between two orientations of the

molecule's TDM. Whereas most of the studied OEP molecules showed absence of a tautomerism process, 7% of the total number of the molecules exhibited slow switching between the two *trans* forms. Thus, for the first time, by imaging the orientation of the single molecule TDM we separately observed the two different *trans* forms. These findings give us a new insight into the excited-state tautomerism process and are of fundamental importance for further applications.

2. Experimental

2.1 Experimental setup

For optical measurements we use a home-build inverted confocal microscope with a high numerical aperture objective lens (NA = 1.25) to detect the orientation of the TDM of single quantum emitters when excited by the doughnut modes. A scheme of the setup is depicted in Fig. 1. As excitation source an optically pumped semiconductor laser at 488 nm or a tunable argon-krypton laser, can be used. After the Gaussian beam of the laser source passed the mode conversion part, the resulting doughnut laser mode is focused on the objective lens onto the sample. The fluorescence of the quantum emitters is collected through the same objective and focused onto the detector. By raster scanning the sample through the focal spot, confocal images arise from the signals detected with an avalanche photo diode (APD). For the spectral analysis of selected emitters a CCD camera can be used. The mode conversion part consists of the mode converter and a pinhole with a diameter of 15 μm . The home-made mode converter was manufactured by cutting two $\lambda/2$ plates in four parts each: one perpendicular and one parallel, the other one shifted by 45° for both slices, with respect to the polarization direction.³¹ Then four of these eight parts (two from each $\lambda/2$ plate) are glued together tilted by 45° towards each other. By turning the mode converter by 90° the polarization of the laser beam between azimuthal and radial polarization can be changed.

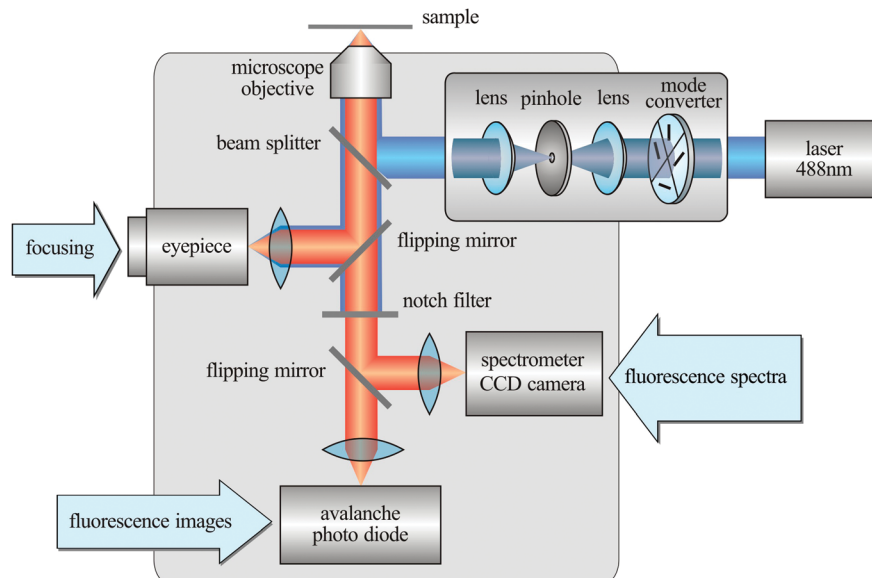


Fig. 1 Scheme of the experimental setup.

The pinhole, placed at the focal point between two lenses, is necessary to cut out other higher order modes which occur due to structural discontinuity at the edges of the $\lambda/2$ plates.

Because of the low quantum yield of the investigated molecules **1** and **2** (Fig. 5) ($\eta = 0.27$ for **1** and $\eta = 0.07$ for **2**), very efficient fluorescence detection is needed. Hence, some measurements of these molecules were performed using a home-built confocal microscope with a parabolic mirror instead of an objective lens as the focusing and light collecting element.³⁷ The advantage of a parabolic mirror over an objective lens is its ability to collect all light in a solid angle of nearly 2π over the sample and in addition it provides well defined polarization states in the focal region when illuminated with RPDM or APDM. For these parabolic mirror experiments a He–Ne laser at 633 nm was used as an excitation source.

2.2 Higher order laser modes

In this section we will briefly describe the theoretical background of mode formation. In general, solving the scalar Helmholtz equation for an electromagnetic field within the boundary conditions of a laser resonator results in stationary solutions, eigen states or what is referred to as modes. Applying the paraxial approximation the solution of these eigen states can be written as so called Hermite-Gauss modes (HG_{mn}) for cartesian coordinates or as Laguerre-Gauss modes (LG_{pl}) for cylindrical coordinates. These eigen states play an important role in optical and laser engineering. The simplest and often the most desirable type of beam provided by a laser source is the Gaussian beam, the fundamental transverse electromagnetic mode TEM_{00} . All types of higher order modes can be described by a linear combination of the Hermite-Gauss or Laguerre-Gauss modes. In general, there are two ways to generate these higher order laser modes: either inside a laser cavity^{38–41} or transforming the Gaussian laser beam extra-cavity using a mode converter. However, for most research areas, the passive generation of higher order laser modes from a Gaussian beam outside the laser resonator delivers an adequate beam quality and is much easier to achieve. The conversion can be realized by different types of mode converters. Liquid crystal mode converters⁴² are convenient when different wavelengths have to be used to examine the sample. If the flexibility in wavelengths is not an issue, APDM and RPDM cylindrical vector beams can be generated from linear polarized light by a special arrangement of $\lambda/2$ wave plates. The mode creation *via* a four-segment mode converter is shown in Fig. 2. Basically, an APDM or RPDM is obtained by combining the TEM_{10} and TEM_{01} modes in the following way:³⁵

$$AP = -HG_{01}n_x + HG_{10}n_y \quad (2)$$

$$RP = HG_{10}n_x + HG_{01}n_y. \quad (3)$$

A further superposition of RPDM and APDM results in the formation of a generalized cylindrical vector beam, which is described nicely in the papers of Zhan and co-workers.^{35,36}

Due to the structural discontinuity at the edges of the segments, different higher order modes are generated of which the undesired modes have to be removed. This mode cleaning

can be done either by a pinhole^{43,44} or by a near-confocal Fabry-Perot interferometer.³¹

Although both beams show free propagation in all polarization states in the x/y -plane perpendicular to the propagation direction z , their behavior changes when they are focused. While the azimuthally polarized beam is composed only of in-plane (x/y) polarization components of the electric field, the radially polarized beam has an additional field component in the z -direction (*cf.* Fig. 3(a)). The rather complex formation of the field distribution of both, APDM and RPDM, in the focus is depicted in Fig. 3(b). The blue arrows represent the situation for the electric field vectors in the focal spot, where all beams travel the same optical path length and the longitudinal field components interfere constructively. For each in-plane vector component in the focal spot exists a complement with an opposite orientation, *i.e.* corresponding fields have an antiparallel orientation, and therefore the resulting in-plane field strength is zero. The red arrows render the situation for a spot which is shifted laterally away from the focus. Now the two beams coming from the lens travel different optical pathways and hence accumulate a phase difference. For a phase shift of π the field vectors have parallel orientation resulting in maximum constructive interference.

The quality of these higher order laser modes is examined by imaging them with fluorescent spheres. These nanometre-sized polystyrene spheres contain a large number of fluorescent molecules (~ 200), where the individual molecules have random orientation. Thus, the sphere acts as an isotropic absorber/emitter and all polarization states of the excitation light are absorbed simultaneously (in contrast to the interaction of these modes with a single transition dipole of one distinct absorber, like a single molecule). Therefore, the scan image is a measure for the electric field distribution in the focus of the excitation beam. The spheres, purchased from Molecular Probes (Leiden Netherlands), have a diameter of 20 nm and are loaded with Nile Red molecules. To probe the modes, a diluted solution of the spheres was spin-coated on a glass substrate. For this experiment either a 488 nm or 514 nm laser was used to excite the dye. The scan images in Fig. 3(c) show the results of the interaction of an azimuthally (left) and a radially (right) polarized mode with an isotropic emitter. In the focus of an APDM the electric field vectors in the focal area are polarized parallel to the surface, exactly like the far field intensity distribution of the beam. Thus, a perfect ring-shaped pattern appears when an isotropic emitter is scanned through the focus of an azimuthal mode. The experimentally obtained scan image and the corresponding calculated pattern for a microscope objective lens with a high numerical aperture (NA) are shown on the left-hand side in Fig. 3(c). In contrast, the focus of a radial mode consists of a very strong field polarized perpendicular to the surface, which is much stronger than the ring of the in-plane field components around it. As a consequence, the excitation pattern mainly presents the interaction with the strong perpendicular field in the center (see Fig. 3(c)).

The interaction of these doughnut modes with the dipole moment of a single quantum emitter is shown in Fig. 4. The purely transversal electric field \vec{E} of an APDM in the focus

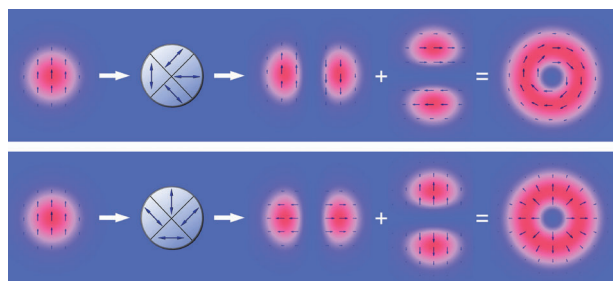


Fig. 2 Scheme of APDM and RPDM generation: a mode converter fabricated by four half-wavelength plates transforms a linear polarized Gaussian beam into the two orthogonal first-order Hermite-Gauss modes, which combine to the ring-shaped higher order modes. Depending on the position of the half-wavelength-plates either an APDM or RPDM is generated.

interacts only with the components of the dipole moment $\vec{\mu}$ which are parallel to the sample plane. As the molecule is much smaller than the focal spot of the laser beam, the transition dipole of the molecule maps the local electric field at different positions in the focal plane during raster scanning, *i.e.* the molecule can only be excited if the polarization in the excitation beam coincides with the projection of the emitter's TDM orientation. In turn, the fluorescence rate R_f of a molecule is given by $R_f \sim |\vec{\mu} \cdot \vec{E}|^2$. Therefore, we efficiently map the excitation pattern of the quantum emitter with an optical resolution higher than the diffraction limit. As a consequence, a molecule oriented with its TDM perpendicular to the sample plane cannot be excited by an APDM (Fig. 4(b), $\theta = 0^\circ$). The further the TDM is turned towards the sample plane, a double-lobe shaped excitation pattern arises. This pattern has its maximum intensity for in-plane orientation of the dipole (Fig. 4(b), $\theta = 90^\circ$).

The RPDM has in addition to the in-plane polarization components also components in the longitudinal direction, and thus, the resulting excitation patterns have shapes ranging from spot-like to double-lobe patterns, depending on the 3D orientation of the dipole moment. From the calculations presented in the lower row of Fig. 4(b) it can be seen that a double-lobe pattern arises from a dipole in the focal plane and changes to a spot-like pattern for a dipole oriented perpendicular to this plane.

2.3 Computational details

Calculations of the electric field distribution in the focal region and the excitation patterns were performed with the “Focused Fields” program by A. Lieb and with a modified version of this program, “PMCalc” (modified by M. Sackrow).⁴⁵ Scan images were processed with the software WSxM of Nanotec.⁴⁶

The quantum chemical calculations were carried out with the Gaussian 03 program.⁴⁷ Optimized geometries, vibrational frequencies and relative energies for the various conformers and tautomers were obtained at the B3LYP/6-311G* level of theory. All structures investigated represent minima on the corresponding energy hypersurface (*i.e.* possess no imaginary frequency). Calculations of the electric TDMs for the first excited electronic state S_1 were performed by applying the RCIS/6-311G*//B3LYP/6-311G* approximation. In the

case of **1** (Fig. 5), additionally the first order transition states (first imaginary frequency) for the tautomerism process *trans*-to-*cis* in the electronic states S_0 and S_1 were obtained. Geometry optimizations for the S_1 structures were performed applying time-dependent density functional theory (B3LYP-TD/6-311G*, see below).

2.4 Molecules

The symmetrically substituted metal-free phthalocyanine (**1**) and porphyrin (**3**), nonsymmetrically substituted porphyrazine (**2**) (Fig. 5) were synthesized according to published procedures.^{48–50} The purity of the compounds was tested using thin layer chromatography. All compounds were characterized by IR-, UV/Vis-, and ^1H NMR-spectroscopy as well as mass spectrometry.

The main difficulty in the current experiments is the fast bleaching of the investigated molecules. Hence, some measurements were performed with a constant soft flow of nitrogen over the sample during the measurement which noticeably reduced the bleaching of the molecule fluorescence. All measurements were performed at room temperature.

2.5 Sample preparation

Using an inverted confocal microscope with an objective lens as a focusing element the samples have to be prepared on thin transparent substrates, like non-fluorescent glass cover slides (here: thickness of 170 μm), which have to be cleaned carefully to avoid any kind of contamination fluorescence. To obtain single molecule concentrations on the sample, solutions of $10^{-9}\text{ mol l}^{-1}$ of molecules **1**, **2**, **3** in dichloromethane or toluene are added to non-fluorescent transparent polymer solutions $\leq 1\%$ and spin coated on the cleaned cover slides. The thickness of these layers is approximately 50 nm as determined by atomic force microscopy (AFM) measurements. The polymer matrix, *e.g.* PMMA (polymethylmethacrylate, $[\text{C}_5\text{O}_2\text{H}_8]_n$) or PS (polystyrene, $[\text{C}_8\text{H}_8]_n$), is used to fix the single emitters on the cover slide. Hence, translation and rotation of the quantum objects are excluded. Depending on the speed of the spin coater (~ 8000 rpm), solutions with concentrations lower than $10^{-9}\text{ mol l}^{-1}$ are needed.

Samples for measurements using a confocal microscope equipped with a parabolic mirror were prepared under clean-room conditions from a $10^{-9}\text{ mol l}^{-1}$ solution of molecules **1** or **2** in toluene onto a silicon surface giving a mean distance $> 1\text{ }\mu\text{m}$ between adjacent molecules. All substrates were previously cleaned with a $\text{H}_2\text{SO}_4/\text{H}_2\text{O}_2$ mixture.

3 Results and discussions

3.1 NH Tautomerization

The molecules, are excited either to a vibronic level, located lower than the barrier (Fig. 6, (1)), separating the *trans* tautomers from the *cis* form, or higher (Fig. 6, (2)). In the first case the molecule recombines to the ground state within the same *trans* tautomer. In the second case it reaches a level, with higher energy than the barrier between the different tautomers, it can transfer to the excited state of another *trans* form, which leads to recombination to the respective ground state.

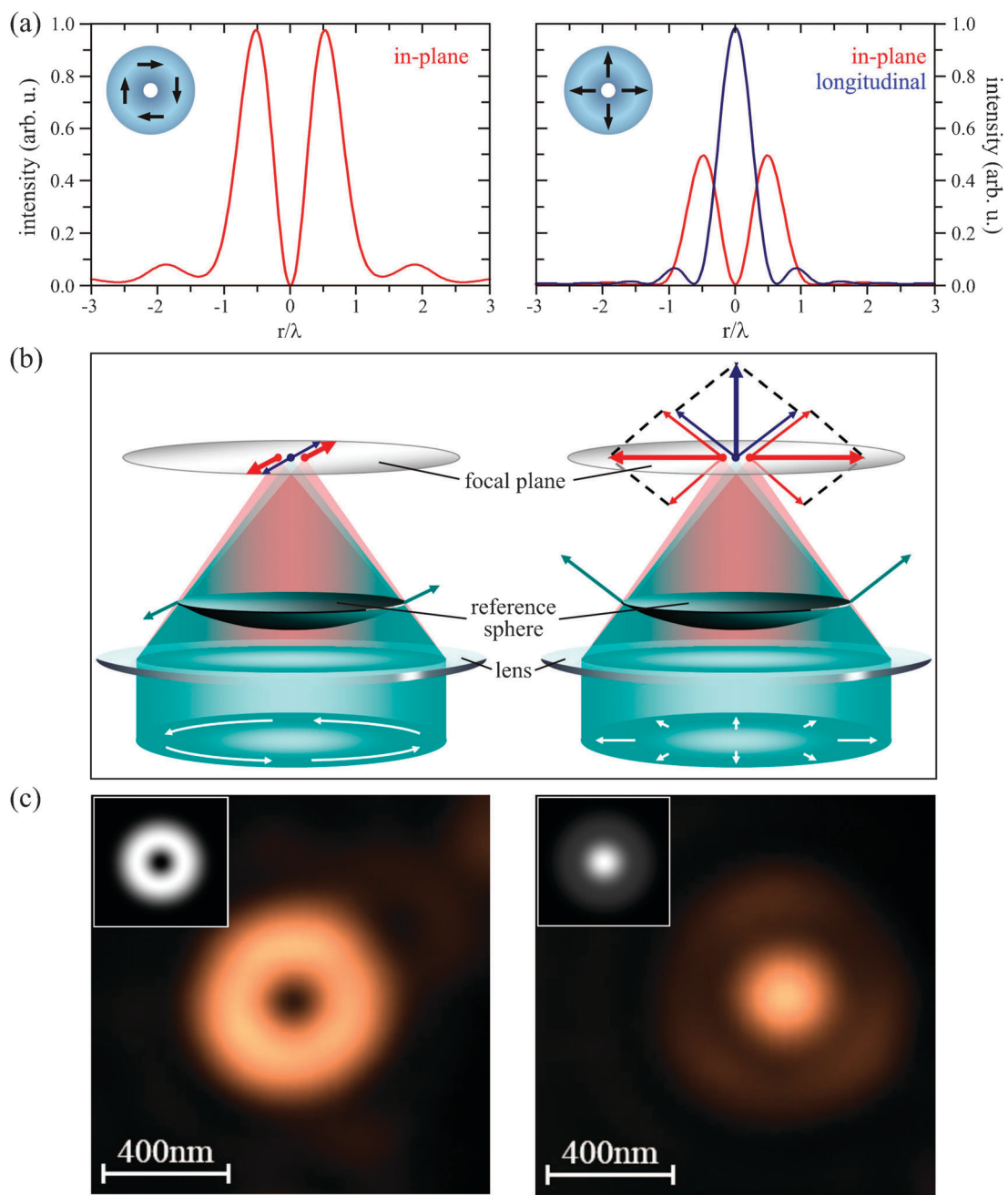


Fig. 3 (a) Calculated intensity distribution of the electromagnetic field in the focus of an APDM and a RPDM. While the APDM (left) possesses only components in the focal plane, the RPDM (right) consists of both in-plane and longitudinal components. The numerical aperture (NA) of the objective lens is 1.25. For other NA values, the intensity ratio of the polarization components varies. (b) Geometrical representation of the electrical field formation of an APDM (left) and a RDPM (right) in the focal volume of a lens. (c) Controlling the quality of the doughnut modes with a single fluorescent sphere by confocal imaging ($\lambda_{\text{exc}} = 488$ nm, NA = 1.25): APDM (left), RPDM (right). The insets show the corresponding calculated intensity distribution.

Two mechanisms of the tautomerism process (2) (Fig. 6) are proposed, a two-step and a single-step. In the two-step mechanism, the two H atoms migrate one after another from the *trans* through a transition state to *cis* and through a transition state to *trans*. The single-step mechanism involves synchronous migration of the two H atoms from *trans* to a transition state and *trans*. The transition state specified is characterized by no N–H bond, but where the two H atoms are equally shared between two N atoms (two intramolecular H-bonding), and

corresponds to the concerted mechanism. According to quantum chemical calculations the two-step mechanism is preferred for H₂Pc as well as for OEP molecules.^{51–53}

3.2 Simulated excitation patterns for different angles between two dipoles and different orientation of the molecule

Scanning a single molecule with distinct orientations of its TDM through the focal region of an APDM results in a

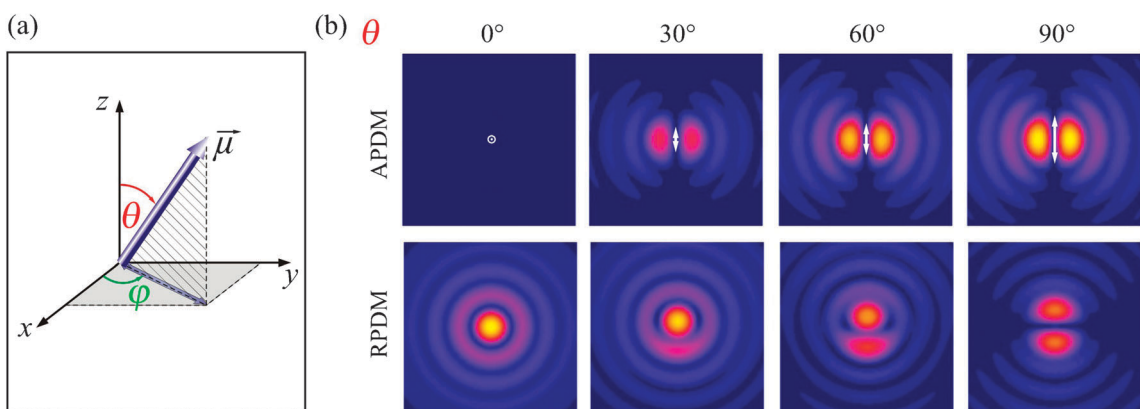


Fig. 4 Interaction of an APDM and a RPDM in the focal spot with a dipole of a quantum emitter: (a) coordinate system of the dipole moment, (b) calculated patterns for different θ angles ($\varphi = 0^\circ = \text{const.}$). The arrows drawn in the patterns resulting from APDM excitation indicate the lengths of the dipole moment's projection onto the x/y -plane.

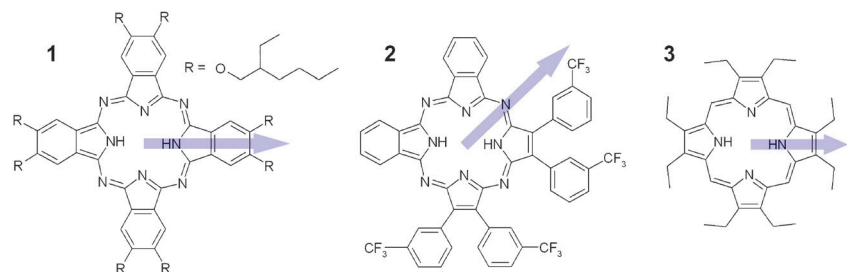


Fig. 5 1: Symmetrically substituted phthalocyanine (H_2Pc); 2: nonsymmetrically substituted porphyrazine; 3: symmetrically substituted porphyrin (OEP). The arrows indicate the calculated transition dipole moments $\vec{\mu}$ for the $S_0 \rightarrow S_1$ transition of the respective *trans* tautomers. The CF_3 -groups in the case of 2 are arranged in “up-down-up-up” positions (see text).

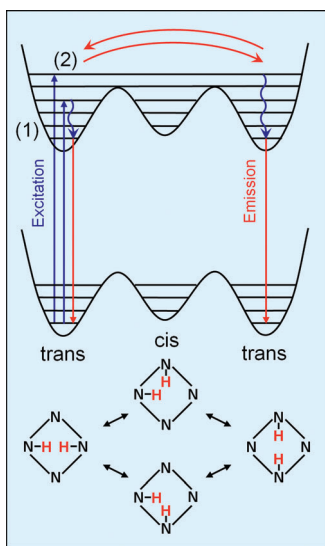


Fig. 6 Scheme of the excited-state tautomerism process.

characteristic double lobe excitation pattern. This pattern (Fig. 7(e)) is given by the projection of the incident field \vec{E} onto the direction of the transition dipole moment $\vec{\mu}$, since the detected fluorescence intensity is proportional to $|\vec{\mu} \cdot \vec{E}|^2$. If the orientation of the TDM changes due to the tautomerism process faster than the acquisition time of one line-scan of the image, a pattern results in a superposition of double lobe

patterns for the respective orientations of their TDMs. Assuming the change in orientation is 90° , the excitation pattern in the scan image would have a doughnut-like shape as depicted in Fig. 7(h). If the angle between the orientations is different from 90° , the doughnut degenerates towards an asymmetrical intensity distribution depicted in Fig. 7(f) and (g). Hence, by fitting such theoretical patterns to the measured fluorescence excitation patterns, the angle enclosed between the TDMs for the two tautomeric forms could be determined for every molecule. However, the accuracy of such an analysis depends on the quality, *i.e.* the signal-to-noise ratio of the experimental data. Comparing our measurements with the theoretical simulations it is possible to clearly distinguish between double-lobe patterns or doughnut patterns if the angle between the transition moments is between 60 and 120° .

Now, assuming that the tautomerism process results in a change of the orientation of a molecule's TDM by 90° we would like to consider how the shape of a single molecule pattern is modified upon the change of the molecule's orientation with respect to the sample surface (Fig. 8(a)–(d)). According to this condition, Fig. 8(e) shows for an APDM a simulated excitation pattern of a horizontally oriented molecule undergoing a tautomerism process. The ring-shaped pattern is a result of the superposition of two double lobe patterns, turned at an angle of 90° with respect to each other. If the molecule is oriented vertically with respect to the sample surface, both projections of the molecule's TDMs on the

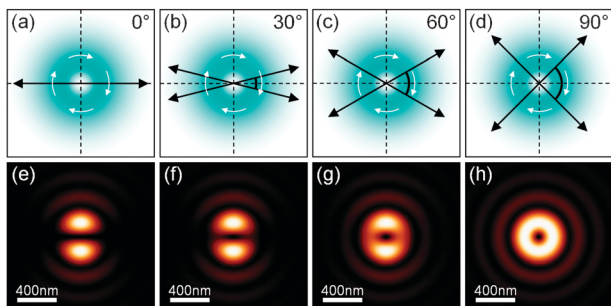


Fig. 7 (a)–(d) Scheme of two transition dipole moments (shown as black arrows), lying in the plane of the sample surface, turned at different angles with respect to each other in the focal area of an APDM focused with a high numerical aperture objective lens or parabolic mirror (the direction of light polarization is shown with white arrows). (e)–(h) Calculated excitation patterns for the superposition of two transition dipole moments with different angles in between, according to schemes (a)–(d), respectively.

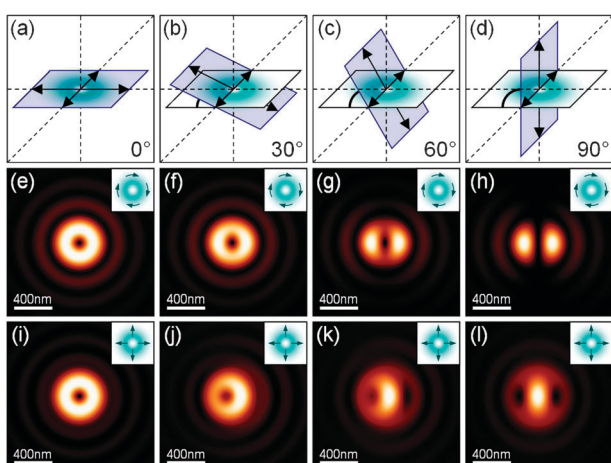


Fig. 8 (a)–(d) Scheme of the molecule possessing two orthogonal transition dipole moments, lying in the plane, shown with blue plane. The molecular plane exhibit different orientation with respect to the sample surface (white plane). Simulated excitation patterns of a single molecule possessing two orthogonal transition dipole moments as a result of the tautomerism process upon excitation with an azimuthally ((e)–(h)) or radially ((i)–(l)) polarized laser beams focused with an objective lens. The molecule is oriented according to scheme (a)–(d).

sample surface are parallel to each other. In this case when the molecule is excited with an APDM, it exhibits the same excitation pattern, as in the case of the fixed linear TDM (*i.e.*, a double lobe pattern, Fig. 8(h)). If the molecule is tilted, the pattern shows a quasi-ring shape (Fig. 8(f) and (g)), which varies depending on the particular orientation.

However, the double lobe pattern can be observed not only in the case of the vertically oriented molecule with fast tautomerization, but also in the absence of the tautomerism process. Recording the excitation patterns of the molecule, excited with a RPDM, which possesses a longitudinal field component, allows one to distinguish between these two cases. A pattern of the vertically oriented molecule with fast tautomerism process, excited with a RPDM, exhibits a prolate spot, in the center of weaker rings (Fig. 8(l)) which can not be

observed upon excitation of the molecule possessing a fixed linear TDM. Horizontally oriented molecules can be excited only with the in-plane field component, therefore, the pattern exhibits a similar doughnut-like shape (Fig. 8(i)), as in the case of the excitation with an APDM. The molecules, which are tilted with respect to the sample surface, show different intermediate asymmetric shapes either resembling a ring-structure (Fig. 8(j)) or a prolate spot (Fig. 8(k)) depending on the particular orientation.

3.3 Phthalocyanine

The phthalocyanine (H_2Pc) **1** (Fig. 5) is symmetrically substituted with ether groups.⁴⁸ The ether groups efficiently prevent aggregation in solution and on surfaces, confirmed by the analysis of position, half-width and shift of the Q-band components in its UV/Vis absorption spectrum.⁴⁸ The position of the two inner ring protons in **1** defines two equivalent tautomeric *trans* forms for the isolated molecule.

In the electronic ground state, according to the B3LYP/6-311G* calculations, the *cis* tautomer is 40.2 kJ mol⁻¹ higher in energy than the *trans* form and the barrier for *trans*-to-*cis* tautomerization is near 58.6 kJ mol⁻¹. These values only slightly change for the corresponding structures in the S_1 state (B3LYP-TD/6-311G*), that is, in both states the *trans* tautomer is predicted to be more stable than the *cis* form.

Quantum chemical calculations (RCIS/6-311G*//B3LYP/6-311G*) show that the angle between the TDMs of the two *trans* tautomeric forms of **1** is 90°. Therefore, at room temperature tautomerization changes the direction of the TDM much faster than the scan speed in the optical measurements (10 ms per image pixel and 198 s per image). When the molecule is raster-scanned through the focus of an APDM focused by parabolic mirror, the optical image (Fig. 9(a)) has a

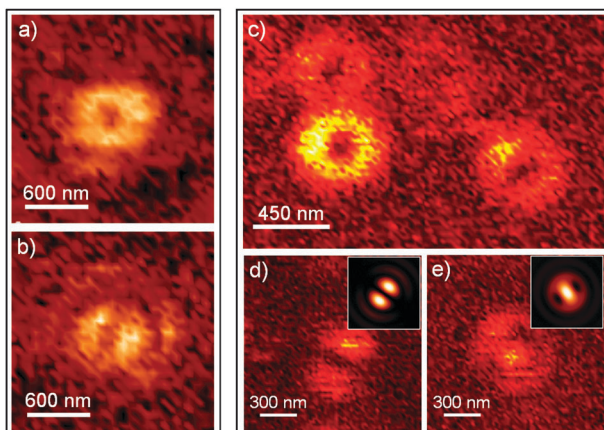


Fig. 9 (a), (b) Scan images of **1** spin coated on a silicon surface without polymer matrix, with an APDM focused by a parabolic mirror with an integration time of 10 ms per pixel. (a) The tautomerization rate is faster than the scan speed. (b) Distorted double lobe pattern, which indicates that the orientation of the molecule is close to vertical. (c) Scan image of three molecules **1** embedded in the polymer matrix and excited with an APDM focused by an objective lens. (d) and (e) Images of the same molecule excited with an APDM and RPDM, respectively, focused by an objective lens. The insets show the corresponding calculated patterns.

doughnut-shape. This is consistent with the images previously presented for porphycene.^{26,27} The image clearly demonstrates that the direction of the TDM changes in the tautomeric process as predicted by the calculations. From 25 observed molecules, 17 show a clear ring shape, however, the other patterns have a distorted shape closer to a double lobe (Fig. 9(b)), suggesting that the orientation of the molecule is close to vertical.

In order to exclude a rotation or movement of **1** on the substrate surface during the scan and to show that molecules, which have double lobe patterns, are vertically oriented with respect to the sample surface, the molecules were embedded in a PMMA matrix. For these measurements a similar home-build confocal microscope equipped with an objective lens instead of a parabolic mirror and an Ar⁺ laser at 488 nm for the excitation were used. The molecules excited with an APDM exhibited both doughnut- and double lobe patterns, as in the case of polymer absence (Fig. 9(c)). To determine the 3D orientation of the molecules showing double lobe fluorescence patterns, we used a RPDM for the excitation.^{28,33} Fig. 9(d) and (e) show the experimental and simulated fluorescence patterns of one molecule **1** excited with APDM and RPDM, respectively. According to simulations described in the section 3.2 these patterns correspond to the molecule which is oriented vertically with respect to the sample surface.

3.4 Porphyrazine

Molecule **2** (Fig. 5) is a porphyrazine derivative of AABB type.⁴⁹ In the optical measurement, no ring-shaped patterns were observed for this kind of molecule. All 35 measured molecules showed clear double lobe patterns (Fig. 10(a) and (b)). The molecule in Fig. 10(b) shows bleaching behavior demonstrating that the single molecules were investigated.

Such double lobe patterns may appear if the molecule does not lay flat on the surface and its TDM possesses a tilted orientation relative to the substrate plane. Focusing a RPDM

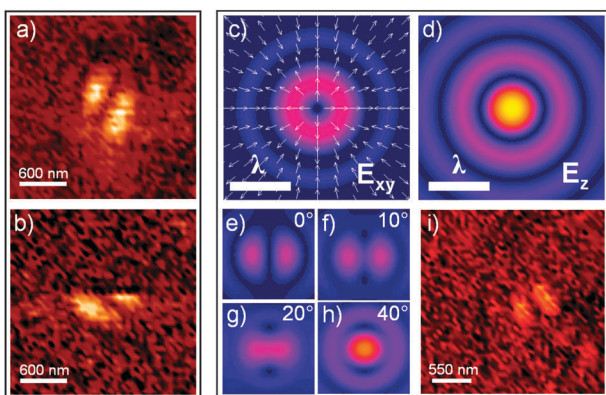


Fig. 10 (a) & (b) Scan images of **2** with azimuthally polarized light, showing clear double lobe patterns. The molecule in (b) was bleached during the scan (scan direction is bottom-up). (c) & (d) Electric field in the plane of the sample and perpendicular to the sample of a calculated focus for a radially polarized laser beam focused by a parabolic mirror, respectively. (e)–(h) Resulting excitation patterns for a dipole with different angles θ to the sample surface, (e) $\theta = 0^\circ$ (f) $\theta = 10^\circ$ (g) $\theta = 20^\circ$ & (h) $\theta = 40^\circ$. (i) Scan of molecule **2** with radially polarized light, demonstrating that the molecule lays flat on the surface.

by a parabolic mirror (Fig. 10(c) and (d)) for excitation, one can in addition obtain information about the orientation of the TDM perpendicular with respect to the surface plane.²⁸ The focus of a RPDM produces a strong electric field component perpendicular to the surface, which would lead to a single bright intensity maximum (Fig. 10(h)) for a molecule **2** that has its TDM in the vertical direction. In measurements performed with the sample of molecule **2** with a RPDM only shallow double lobe excitation patterns were observed (Fig. 10(i)), which result from the interaction of the TDM with the weak in-plane field components (Fig. 10(c)). Thus, we conclude that the molecules essentially are oriented parallel to the sample surface.

A clear double lobe pattern can be expected either when only one tautomeric form is present during one scan or when the TDMs of the two tautomers form an angle lower than 60° or higher than 120° . Both hypotheses have to be cross-checked with theoretical calculations.

Quantum chemical calculations (B3LYP/6-311G*) show that in **2** the central ring is slightly bent, which is due to the orientation of the phenyl substituents carrying each one CF₃ group. The trifluoromethylphenyl groups are rotated out of plane of the chromophoric ring with calculated angles of 37° to 55°. The CF₃ groups can be arranged over (up) or below (down) the porphyrazine ring. The calculations also predict, that the “up-down-up-down” (udud) and the “up-down-up-up” (udu) species represent the most stable conformers (*trans* tautomers) being equal in energy. The four other possible conformations (*trans* tautomers, *i.e.* uudd, uuuu, duud and uuud) are higher in energy by about 4.5 to 11.7 kJ mol⁻¹. The rotations of the phenyl rings are strongly hindered, therefore, it is expected that the molecule is frozen in one conformation, which is either udud or uduu. The calculated energy differences between the respective *trans* and *cis* tautomers in the udud and uduu forms of **2** vary from 34.8 to 55.1 kJ mol⁻¹ with the *cis* structure being higher in energy than the *trans* tautomers in all cases. The energy differences depend on the orientation of the CF₃ groups and on the structure of the respective *cis* tautomer: for each of the six possible *trans* tautomers four different *cis* tautomers are conceivable. Hence, the tautomerization should be much faster at room temperature than the scan speed of the measurement. On the other hand, the angles between the TDMs of the corresponding *trans* and *cis* tautomers of the udud and uduu structures are predicted to lay in the ranges of 5° to 30° or 140° to 170°. In accordance with the simulations presented in Fig. 7, these angles are in that range, where the excitation pattern still has a clear double lobe shape which makes it difficult to detect the tautomerism process. The energies of the structures are summarized in the ESI.†

3.5 Porphyrin

The octaethylporphyrin (OEP) is a symmetrically substituted molecule (Fig. 5). According to quantum chemical calculations the angle between the TDMs of the two *trans* forms of the OEP molecule is 90°. According to the B3LYP/6-311G* calculations the *cis* tautomer is about 37.6 kJ mol⁻¹ less stable than the *trans* structure, therefore the molecule in the electronic ground state S₀ can only be in one of the two *trans* forms.

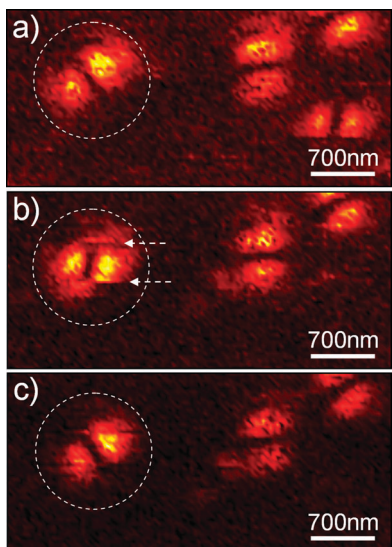


Fig. 11 (a)–(c) Images of single OEP molecules embedded in a PMMA matrix and excited with an azimuthally polarized laser beam; the images were recorded one after the other. The molecule in the white dashed circle shows a change of the TDM orientation. The acquisition time of one image is 400 s. The scan direction is top-down. Image (b) shows the sudden flipping of the TDM, caused by the transition of the molecule from one *trans* form to another. Two arrows show the part of the image (corresponds to 36 s acquisition time), where the molecule possesses a fixed orientation of the TDM, *i.e.*, stays in the same *trans* form.

And for this reason, the molecule can be excited only from one of the chemically equivalent *trans* tautomers.

In contrast to the investigated H₂Pc molecules, OEP molecules show no ring-like shaped patterns after the excitation with an APDM. Most of the investigated molecules exhibit stable double lobe fluorescence patterns, while only 7% of the molecules show flipping of the TDM. In Fig. 11 a series of fluorescence images of four single OEP molecules excited with an APDM is presented. The images were recorded one after the other. The molecule in the white dashed circle shows a sudden change of the TDM orientation during the scan (Fig. 11(b)), while the other molecules possess stable excitation TDMs. Two arrows in the Fig. 11(b) show where the TDM of the molecule flipped from one orientation to another, *i.e.*, the molecule switched between two *trans* tautomers. From the image we estimated that the time, when the molecule was in the same *trans* form (the central part of the pattern between the arrows) is 36 s. In Fig. 11(c) the molecule has the original TDM orientation like in Fig. 11(a).

Since the OEP molecule can be excited only from one of the *trans* structures (but not from the less stable *cis* form), the excitation pattern reflects the orientation of the TDM of the molecule in the *trans* forms. The angle between two TDM orientations of the molecule in the white circle (Fig. 11(a) and (b)) is less than 90°, which is different from the result of the quantum chemical calculations. This can be explained by the fact that the pattern obtained upon excitation of the molecule by an APDM shows the projection of the TDM on the sample surface. Therefore, if the molecule is tilted with respect to the

sample surface, the angle between two projections of the TDMs of the molecule in the *trans* tautomers is less than 90°.

In Fig. 12 an image series of the same single OEP molecule excited with an APDM is depicted. The pattern in Fig. 12(a) demonstrates the flipping of the TDM during the scan. The upper and lower parts of the image correspond to the TDM orientation like in Fig. 12(b), while the middle part corresponds to the TDM orientation like in Fig. 12(c). Since the molecule can be excited only from one of the two *trans* forms, the measured patterns correspond to the different *trans* tautomers of the single molecule. The angle between the two TDM projections is nearly 90° (Fig. 12(b) and (c)), thus the molecule is lying parallel to the sample surface.

Thus, for the first time we could observe that a molecule undergoing a tautomerism process stays in one tautomeric *trans* structure during time comparable with the acquisition time of one excitation pattern (*i.e.*, near 400 s). This allowed us to visualize the existence of each of the two *trans* forms of a single OEP molecule, as well as the sudden switching between these tautomers. Such observations are impossible for molecules, where the switching between the *trans* structures occurs faster than the acquisition time of one line of the excitation pattern (for example, H₂Pc molecules).

We investigated molecules embedded in polar (PMMA) and nonpolar (PS) polymers directly spin coated on the surface of the cover slide and found qualitatively the same behavior.

4. Conclusions and perspectives

In summary, we showed that cylindrical vector beams focused with a high NA objective lens or parabolic mirror can be used to image the tautomerism process in spatially isolated and immobilized single phthalocyanine (**1**), porphyrazine (**2**) and porphyrin (**3**) molecules. This method allowed us to distinguish between the fast and slow (with respect to the acquisition time of one line-scan of the single molecule fluorescence image) tautomerism process at the single molecule level. Using a RPDM we determined the three dimensional orientation of an individual molecule by comparing the experimental and simulated excitation patterns. The recorded excitation patterns exhibited the usual fluorescence dynamics such as blinking and bleaching, clearly indicating that single molecules

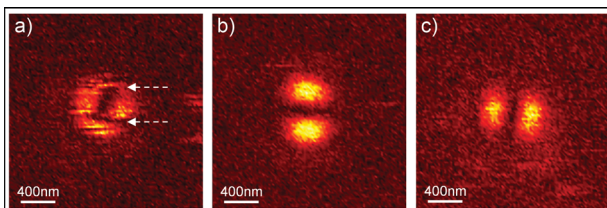


Fig. 12 (a)–(c) The image series of a (same as in the text) single OEP molecule embedded in a PMMA matrix and excited with an azimuthally polarized laser beam; the pictures were recorded one after the other. The acquisition time of one image is 400 s. The scan direction is top-down. (a) Tautomerization occurs twice during the scan process. As indicated by the arrows, the central part of the image (corresponds to 30 s acquisition time) shows the fixed TDM orientation of the molecule in one of the *trans* forms. (b), (c) Excitation patterns of both *trans* forms of the same single OEP molecule.

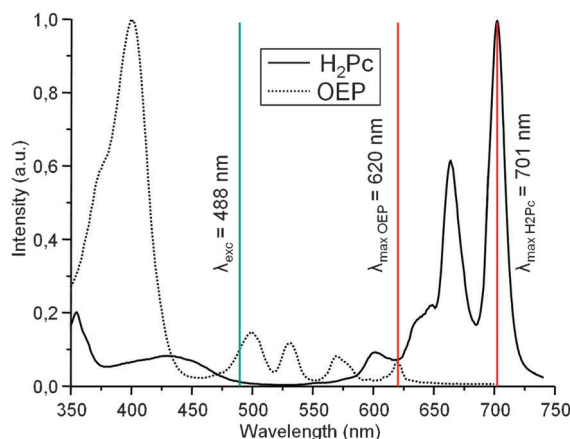


Fig. 13 Excitation spectra of H₂Pc and OEP molecules (**1** and **3**, respectively). The plot shows the excitation wavelength (green line) and maxima of the most red-shifted spectral bands (red lines).

were studied. By comparing the experimental and simulated single molecule patterns upon excitation with an APDM we showed that the quantum chemical calculations are in a very good agreement with obtained results.

In particular, the phthalocyanine molecules **1** exhibited either doughnut-shaped excitation patterns, suggesting a fast tautomerism process between two *trans* forms with TDMs forming an angle of 90°, or double lobe patterns, corresponding to a tilted orientation of the molecule with respect to the sample surface.

The patterns of the asymmetrically substituted porphyrazine molecules **2** showed only the double lobe structure, excluding tautomerism with a turn of the TDM to 90°. This result is in good agreement with the quantum chemical calculations, which predict a change of the TDM orientation within the ranges from 5° to 30° or from 140° to 170°. In this case the molecule is expected to render double lobe patterns that are difficult to distinguish from a single dipole moment orientation.

Most of the investigated single porphyrin molecules **3** show a stable TDM and only for 7% of the total number of molecules a sudden flipping of the TDM orientation between two *trans* tautomers was observed. Thus, for the first time we are able to detect the two *trans* forms separately. According to the quantum chemical calculations, the angle between TDM orientations of the two *trans* forms is 90°. Therefore, the double lobe pattern, which was obtained upon excitation of 93% of the total number of the molecules with an APDM, can be observed either in the case of the absence of the tautomerization or in the rare case of a vertical orientation of the molecule with a tautomerism process. We relate the absence of the tautomerism process (fixed orientation of the single molecule excitation pattern) to the following reasons: (1) The energy barrier between *trans* and *cis* forms is too high. Therefore, the molecule is always excited from the same *trans* form in the ground state. (2) The excitation energy 245 kJ mol⁻¹ at the laser wavelength (488 nm) is not high enough to overpass the energy barrier between the two tautomeric forms in the excited state potential of OEP molecules. The absorption maximum of the OEP molecules is at 400 nm. Assuming that the barrier between the *trans* and *cis* forms of the ground state is not

higher than the barrier in the excited state, let us estimate the energy, which molecules **1** and **3** require for the excited state tautomerism process. It can be estimated as a sum of the barrier energy and the energy corresponding to the maximum of the most red-shifted band in the excitation spectrum of the molecules (Fig. 13). Compared to the excitation energy (245 kJ mol⁻¹), this value determines the possibility for the excited state tautomerism to occur. Thus, for molecule **1** we obtained 228 kJ mol⁻¹, which allows the molecule to undergo excited state tautomerization upon excitation with 488 nm laser light, while molecule **3** showed the value 250 kJ mol⁻¹. The latter exceeds the excitation power, however the energy difference of the order of 5 kJ mol⁻¹ can be compensated by the environment-induced effects, such as local heating or fluctuation of the charges distribution, which leads to the rare sudden switching of the molecule **3** from one *trans* tautomeric form to another.

To obtain more detailed information on this interesting issue, dedicated studies, including spectroscopic measurements as well as imaging of the tautomerism process for the same single molecules will be carried out in the near future.

Acknowledgements

We acknowledge Dr S. Vagin and Dr M. J. F. Calvete for providing the molecules **1** and **2**. We thank Dr H.-J. Egelhaaf and Dr J. Gierschner for their support and stimulating discussions. We gratefully acknowledge financial support from the DFG (ME 1600/5-2), the Landesforschungsschwerpunktprogramm Baden-Württemberg and the European Commission through the Human Potential Program (Marie-Curie Research Training Network NANOMATCH, Contract No. MRTN-CT-2006-035884). We also thank Coherent GmbH Germany for providing a SapphireTM 488-20 OPS laser.

References

- 1 P. Gregory, *J. Porphyrins Phthalocyanines*, 2000, **4**, 432.
- 2 M. Ochsner, *J. Photochem. Photobiol., B*, 1997, **39**, 1.
- 3 D. Phillips, *Pure Appl. Chem.*, 1995, **67**, 117.
- 4 J. J. Schuitmaker, P. Baas, H. L. L. M. van Leengoed, F. W. van der Meulen, W. M. Star and N. van Zandwijk, *J. Photochem. Photobiol., B*, 1996, **34**, 3.
- 5 I. Lanzo, N. Russo and E. Sicilia, *J. Phys. Chem. B*, 2008, **112**, 4123.
- 6 A. Renn, U. P. Wild and A. Rebane, *J. Phys. Chem. A*, 2002, **106**, 3045.
- 7 www.porphyrin-systems.de (14.05.2009).
- 8 B. Wehrle, H. H. Limbach, M. Köcher, O. Ermer and E. Vogel, *Angew. Chem., Int. Ed. Engl.*, 1987, **26**, 934.
- 9 Y.-D. Wu, K. W. K. Chan, C.-P. Yip, E. Vogel, D. A. Plattner and K. N. Houk, *J. Org. Chem.*, 1997, **62**, 9240.
- 10 H. H. Limbach, J. M. Lopez and A. Kohan, *Philos. Trans. R. Soc. London, Ser. B*, 2006, **361**, 1399.
- 11 M. J. Crossley, M. M. Harding and S. Sternhell, *J. Org. Chem.*, 1988, **53**, 1132.
- 12 J. Braun, R. Schwesinger, P. G. Williams, H. Morimoto, D. E. Wemmer and H. H. Limbach, *J. Am. Chem. Soc.*, 1996, **118**, 11101.
- 13 J. Braun, H.-H. Limbach, P. G. Williams, H. Morimoto and D. E. Wemmer, *J. Am. Chem. Soc.*, 1996, **118**, 7231.
- 14 M. J. Crossley, M. M. Harding and S. Sternhell, *J. Am. Chem. Soc.*, 1986, **108**, 3608.
- 15 M. J. Crossley, L. D. Field, M. M. Harding and S. Sternhell, *J. Am. Chem. Soc.*, 1987, **109**, 2335.

- 16 A. Vdovin, J. Waluk, B. Dick and A. Slenczka, *ChemPhysChem*, 2009, **10**, 761.
- 17 P. Fita, N. Urbanska, C. Radzewicz and J. Waluk, *Chem.–Eur. J.*, 2009, **15**, 4851.
- 18 J. Waluk and E. Vogel, *J. Phys. Chem.*, 1994, **98**, 4530.
- 19 M. Drobizhev, N. S. Makarov, A. Rebane, G. de la Torre and T. Torres, *J. Phys. Chem. C*, 2008, **112**, 848.
- 20 S. Völker and J. H. van der Waals, *Mol. Phys.*, 1976, **32**, 1703.
- 21 U. Even and J. Jortner, *J. Chem. Phys.*, 1982, **77**, 4391.
- 22 K. M. Merz Jr. and C. H. Reynolds, *J. Chem. Soc., Chem. Commun.*, 1988, 90–92.
- 23 J. Jasny and J. Sepiol, *Chem. Phys. Lett.*, 1997, **273**, 439.
- 24 M. Böhmer and J. Enderlein, *J. Opt. Soc. Am. B*, 2003, **20**, 554.
- 25 S. A. Empedocles, R. Neuhauser and M. G. Bawendi, *Nature*, 1999, **339**, 126.
- 26 H. Piwonski, C. Stupperich, A. Hartschuh, J. Sepiol, A. Meixner and J. Waluk, *J. Am. Chem. Soc.*, 2005, **127**, 5302.
- 27 H. Piwonski, A. Hartschuh, N. Urbanska, M. Pietraszkiewicz, J. Sepiol, A. J. Meixner and J. Waluk, *J. Phys. Chem. C*, 2009, **113**, 11514.
- 28 L. Novotny, M. R. Beversluis, K. S. Youngworth and T. G. Brown, *Phys. Rev. Lett.*, 2001, **86**, 5251.
- 29 A. M. Chizhik, A. I. Chizhik, R. Gutbrod, A. J. Meixner, T. Schmidt, J. Sommerfeld and F. Huisken, *Nano Lett.*, 2009, **9**, 3239.
- 30 S. Bär, A. I. Chizhik, R. Gutbrod, F. Schleifenbaum, A. M. Chizhik and A. J. Meixner, *Anal. Bioanal. Chem.*, 2009, **396**, 3.
- 31 R. Dorn, S. Quabis and G. Leuchs, *Phys. Rev. Lett.*, 2003, **91**, DOI: 10.1103/PhysRevLett.91.233901.
- 32 A. V. Failla, H. Qian, H. Qian, A. Hartschuh and A. J. Meixner, *Nano Lett.*, 2006, **6**, 1374.
- 33 A. M. Chizhik, T. Schmidt, A. I. Chizhik, F. Huisken and A. J. Meixner, *Proc. SPIE–Int. Soc. Opt. Eng.*, 2009, **7393**, 739305.
- 34 R. Gutbrod, D. Khoptyar, M. Steiner, A. M. Chizhik, A. I. Chizhik, S. Bär and A. J. Meixner, *Nano Lett.*, 2010, **10**, 504.
- 35 Q. Zhan and J. R. Leger, *Opt. Express*, 2002, **10**, 324.
- 36 Q. Zhan, *Adv. Opt. Photonics*, 2009, **1**, 1.
- 37 C. Stanciu, M. Sackrow and A. J. Meixner, *J. Microsc.*, 2008, **229**, 247.
- 38 K. Yonezawa, Y. Kozawa and S. Sato, *Opt. Lett.*, 2006, **31**, 2151.
- 39 J. F. Bisson, J. Li, K. Ueda and Y. Senatsky, *Opt. Express*, 2006, **14**, 3304.
- 40 M. A. Ahmed, A. Voss, M. M. Vogel and T. Graf, *Opt. Lett.*, 2007, **32**, 3272.
- 41 V. G. Niziev, R. S. Chang and A. V. Nesterov, *Appl. Opt.*, 2006, **45**, 8393.
- 42 M. Stalder and M. Schadt, *Opt. Lett.*, 1996, **21**, 1948.
- 43 A. V. Failla, S. Jäger, T. Züchner, M. Steiner and A. J. Meixner, *Opt. Express*, 2007, **15**, 8532.
- 44 L. Novotny and B. Hecht, *Principles of Nano-Optics*, Cambridge University Press, Cambridge, UK, 2006.
- 45 M. A. Lieb, *PhD Thesis*, University of Siegen, 2001.
- 46 I. Horcas, R. Fernandez, J. M. Gomez-Rodriguez, J. Colchero, J. Gomez-Herrero and A. M. Baro, *Rev. Sci. Instrum.*, 2007, **78**, 013705.
- 47 M. J. Frisch, G. W. Trucks, H. B. Schlegel, G. E. Scuseria, M. A. Robb, J. R. Cheeseman, J. A. Montgomery, Jr., T. Vreven, K. N. Kudin and J. C. Burant, *et al.*, *GAUSSIAN 03 (Revision E.01)*, Gaussian, Inc., Wallingford, CT, 2004.
- 48 M. J. F. Calvete, *PhD Thesis*, University of Tübingen, 2004.
- 49 S. I. Vagin and M. Hanack, *Eur. J. Org. Chem.*, 2002, (16), 2859.
- 50 N. S. Dudkina, P. A. Shatunov, E. M. Kuvshinova, S. G. Pukhovskaya, A. S. Semeikin and O. A. Golubchikov, *Russ. J. Gen. Chem.*, 1998, **68**, 1955.
- 51 T. Strenalyuk, S. Samdal and H. V. Volden, *J. Phys. Chem. A*, 2008, **112**, 4853.
- 52 D. K. Maity and T. N. Truong, *J. Porphyrins Phthalocyanines*, 2001, **5**, 289.
- 53 K. A. Nguyen and R. Pachter, *J. Phys. Chem. A*, 2000, **104**, 4549.